DOI:10.1158/0008-5472.CAN-10-3738

Hedgehog Overexpression Is Associated with Stromal Interactions and Predicts for Poor Outcome in Breast Cancer

Sandra A. O'Toole[1,3,5,6], Dorothy A. Machalek[1], Robert F. Shearer[1], Ewan K.A. Millar[1,8,9,10], Radhika Nair[1], Peter Schofield[2,3], Duncan McLeod[10,11], Caroline L. Cooper[5], Catriona M. McNeil[1,7], Andrea McFarland[1], Akira Nguyen[1], Christopher J. Ormandy[1,3], Min Ru Qiu[4], Brian Rabinovich[13], Luciano G. Martelotto[12], Duc Vu[12], Gregory E. Hannigan[12], Elizabeth A. Musgrove[1,3], Daniel Christ[2,3], Robert L. Sutherland[1,3], D. Neil Watkins[12], and Alexander Swarbrick[1,3]

Abstract

Hedgehog (Hh) signaling plays an important role in several malignancies but its clinical significance in breast cancer is unclear. In a cohort of 279 patients with invasive ductal carcinoma of the breast, expression of Hh ligand was significantly associated with increased risk of metastasis, breast cancer-specific death, and a basal-like phenotype. A paracrine signature, encompassing high epithelial Hh ligand and high stromal Gli1, was an independent predictor for overall survival in multivariate analysis. In 2 independent histological progression series ($n = 301$), Hh expression increased with atypia. Hh ligand overexpression in a mouse model of basal breast cancer increased growth, induced a poorly differentiated phenotype, accelerated metastasis, and reduced survival. A stromal requirement for these effects was supported by the lack of similar Hh-mediated changes *in vitro*, and by stromal-specific expression of *Hh* target genes *in vivo*. Furthermore, inhibition of Hh ligand with a monoclonal antibody (5E1) inhibited tumor growth and metastasis. These data suggest that epithelial–stromal Hh signaling, driven by ligand expression in carcinoma cells, promotes breast cancer growth and metastasis. Blockade of Hh signaling to peritumoral stromal cells may represent a novel therapeutic approach in some basal-like breast cancers. *Cancer Res; 71(11); 4002–14. ©2011 AACR.*

Introduction

The decrease in deaths from breast cancer over the last 2 decades reflects improvements in early detection, and the success of targeted therapies such as tamoxifen in hormone receptor positive disease (1). Recent data show that therapeutic targeting of the HER2 receptor is also making an impact in breast cancer mortality (2). However, in women with basal-like breast cancer, an aggressive subtype lacking expression of the estrogen receptor (ER), progesterone receptor (PR), and HER2, the prognosis remains poor (3). At present, there is a shortage of targetable signaling pathways in basal-like breast cancer.

Several studies have suggested a role for hedgehog (Hh) signaling in breast cancer (4–6). This pathway is a highly conserved developmental signaling system essential for epithelial to mesenchymal signaling in development (7). Deregulation of Hh signaling has been implicated in the pathogenesis of carcinoma, in part through the promotion of epithelial–stromal interactions (8–10).

The Hh ligands, Sonic (Shh), Indian (Ihh), and Desert (Dhh) hedgehogs bind to and inactivate the transmembrane receptor Patched (Ptch). Ptch is a constitutive inhibitor of Smoothened (Smo), a transmembrane protein required for all Hh signaling. In its inactive state, Smo permits the formation of a multiprotein complex that constitutively processes the Gli proteins (Gli1–3) to short, transcriptionally repressive forms. Activation of Smo decouples this complex from microtubule domains and leads to stabilization of full length, transactivating Gli proteins that initiate transcription of *Hh* target genes, including *Ptch*, *Gli1*, and *Hedgehog interacting protein* (Hhip; ref. 7). Expression of these transcripts can be used as an indirect measure of canonical

Authors' Affiliations: [1]Cancer Research and [2]Immunology Programs, Garvan Institute of Medical Research; [3]St Vincent's Clinical School, Faculty of Medicine, University of New South Wales; and [4]Department of Anatomical Pathology, SydPath, St Vincent's Hospital, Darlinghurst; [5]Department of Tissue Pathology and Diagnostic Oncology, Royal Prince Alfred Hospital; [6]Central Clinical School, University of Sydney; and [7]Department of Medical Oncology, Sydney Cancer Centre, Royal Prince Alfred Hospital, Camperdown; [8]Department of Anatomical Pathology, South Eastern Area Laboratory Service, St George Hospital, Kogarah; [9]School of Medical Sciences, University of New South Wales, Kensington; [10]School of Medicine, University of Western Sydney, Campbelltown; and [11]Department of Tissue Pathology, Institute of Clinical Pathology and Medical Research, Westmead, NSW; and [12]Monash Institute of Medical Research, Monash University, Clayton, Victoria, Australia; and [13]Experimental Diagnostic Imaging, UT MD Anderson Cancer Center, Houston, Texas

Note: Supplementary data for this article are available at Cancer Research Online (http://cancerres.aacrjournals.org/).

Corresponding Author: Alexander Swarbrick, Cancer Research Program, Garvan Institute of Medical Research, 384 Victoria St, Darlinghurst, NSW 2010, Australia. Phone: 61-2-9295-8366; Fax: 61-2-9295-8321; E-mail: a.swarbrick@garvan.org.au or D. Neil Watkins, Monash Institute of Medical Research, Monash University, 27-31 Wright St, Clayton, Victoria 3186, Australia. E-mail: neil.watkins@monash.edu

doi: 10.1158/0008-5472.CAN-10-3738

©2011 American Association for Cancer Research.

Downloaded from cancerres.aacrjournals.org on September 19, 2011
Copyright © 2011 American Association for Cancer Research

DOI:10.1158/0008-5472.CAN-10-3738

Hh signaling (10), although Gli1 can be driven by non-Hh–dependent mechanisms (11).

Early reports suggesting Hh signaling may contribute to breast carcinogenesis came through the studies of Lewis and colleagues in mice with heterozygous disruption of *Ptch1* which showed marked abnormalities in mammary ductal structures resulting in hyperplasias and dysplasias similar to human breast lesions (12). More recently members of the same group (13) studying mice with constitutive activation of human Smo under control of the mouse mammary tumor virus (MMTV) promoter, found that mammary ductal cells showed increased proliferation, altered differentiation, and developed ductal dysplasias. This group had also previously shown that mammary ducts of mice with loss of *Gli2* had a range of histological alterations similar to micropapillary ductal hyperplasia in the human breast (14). Tissue recombination studies showed that the role of Gli2 is particular to the stroma, as these duct changes were not seen when epithelium with *Gli2* deleted was transplanted into wild-type mouse stroma, supporting a critical compartmentalization of Hh signaling in development and proliferative mammary ductal lesions.

Although several studies suggest that deregulation of Hh signaling might be important in breast cancer (4, 6, 12–16), the clinical and functional significance of these findings and their potential therapeutic impact is unclear. Therefore, we carried out a detailed immunohistochemical study using rigorously validated antibodies against Hh ligand (the initiating signal), Ptch1 (the pathway receptor), and Gli1 (a widely accepted readout of active canonical signaling) in large, well-characterized cohorts of invasive ductal carcinoma and premalignant and proliferative breast lesions. We also employed a mouse model of mammary carcinogenesis to show that Hh ligand overexpression promotes stromal-dependent tumor growth. Finally, we show that use of a Hh-ligand blocking antibody reduces tumor growth and pulmonary metastases, supporting a functional role of the Hedgehog pathway in breast cancer development and progression.

Materials and Methods

Patients

Three cohorts of patients were used as follows: first, the Garvan/St Vincent's Hospital outcome series (17–19) of 292 patients with invasive ductal carcinoma, and 2 independent cohorts of a histological progression series; the Garvan Institute/St Vincent's Hospital progression series (GSVH-PS) consisting of a subset of 79 patients for whom tissue was still available, from a larger series originally (20) and the Garvan Institute/Royal Prince Alfred Hospital with 222 patients diagnosed with invasive ductal carcinoma (IDC) or ductal carcinoma *in situ* (DCIS) described in an earlier report (21). Ethics approval was granted for the use of pathology specimens and cognate clinicopathologic data (HREC SVH H94/080, SVH H00036, and RPAH X05-0115).

Antibodies and immunohistochemistry

To ensure the specificity of Hh pathway antibodies, rigorous antibody validation was carried out. Immunohistochemistry for Hh pathway antibodies was carried out on a DAKO autostainer using the following antigen retrieval protocols after dewaxing and rehydration: Hh ligand H-160 sc-9024, Santa Cruz, 1:80, 20 minutes in a boiling waterbath in Dako retrieval solution S2367; Ptch1 ab27529, Abcam, 1:50 antigen retrieval for 20 minutes boiling waterbath in Dako retrieval solution S2367 and Gli1, sc-20687, Santa Cruz, 1:100, antigen retrieval 30 seconds at maximum temperature and pressure in a DAKO pressure cooker in DAKO solution s1699. Full details of the protocols for immunohistochemistry are shown in Supplementary Table S1. These antibodies were rigorously validated with robust controls as shown in Supplementary Figures S1–3.

For each marker, 2 specialist breast pathologists (S.A. O'Toole and either D. McLeod, E.A.K. Millar, M.R. Qiu, or C.L. Cooper) independently calculated the percentage staining and the predominant intensity on a predetermined scale of 0: no staining to 3: strong staining in both the epithelial cells of the lesions and the adjacent stroma for each Hh pathway protein (and for Gli1 both nuclear and cytoplasmic expressions were scored). Each core had an H score that was generated by multiplying these scores (17–19, 21).

Intrinsic breast cancer subtypes were assessed immunohistochemically using criteria similar to those recently described by Cheang and colleagues (22) but using FISH to determine *HER-2* status (19). Details for antibodies, immunohistochemistry, *in situ* hybridization, and scoring for these markers, have been previously reported in the invasive ductal carcinoma cohort (17–19, 21).

Immunofluorescence

Immunofluorescence (IF) was carried out on 7-μm-thick mouse tumor samples fixed in 4% (w/v) paraformaldehyde, blocked for 90 minutes with 2% (v/v) horse serum, and incubated with primary antibody (Hhip rabbit H-280 Santa Cruz sc-25465, 1:200) and vimentin (chicken, 50-264, Pro Sci, 1:200). Secondary antibodies Alexa555 Cy3 (red) fluorophore conjugated anti-rabbit 1:300 (A-31572, Molecular Probes) or Alexa488 Cy2 (green) fluorophore conjugated anti-guinea pig (A-11073, Molecular Probes) 1:500 were applied to the sections and incubated for 1 hour in the dark at room temperature. Coverslips were mounted onto slides using Vectashield mounting medium with 6-diamidino-2-phenylindole (DAPI) counterstain (H-1500, Vector Laboratories). Slides were imaged immediately using a Zeiss Axioplan upright fluorescence microscope with Zeiss Axiocam MRm digital camera. Digital images were captured using Axiovision V 4.8.1.0 software.

Animals

All experiments involving mice were carried out under the supervision and in accordance with the regulations of the Garvan/St Vincent's Animal Ethics Committee (Approval 08/41). C3(1)/SV40 large T transgenic mice inbred on FVBN background was obtained from Dr. Jeff Green (NIH). Inbred mice were obtained from the Animal Resource Centre, Western Australia (BALB/c, $Rag^{-/-}$).

Mammary gland transplantation. For the 4T1 model the fourth fat pad of 28-day-week old female BALB/c mice was

Downloaded from cancerres.aacrjournals.org on September 19, 2011
Copyright © 2011 American Association for Cancer Research

DOI:10.1158/0008-5472.CAN-10-3738

surgically visualized and 1×10^6 cells (10 μL) injected. For the M6-SHH/Vector transplants, 0.75×10^6 cells (10 μL) were surgically injected via direct visualization into the fourth fat pad of 21-day-old $Rag^{-/-}$ mice.

In vivo *imaging*. Animals were imaged twice weekly. Briefly mice were first injected intraperitoneally with 200 μL of 30% D-luciferin (diluted from 10 mg/mL in PBS, 6160-80-1 GoldBio) and imaged under anesthesia in a Xenogen IVIS 200 biophotonic imager. Luminescence is expressed as photons/sec/ROI (region of interest) minus background luminescence for a similarly sized region.

Cell lines

M6 mouse mammary carcinoma cells derived from the C3 (1)/SV40 Tag mouse model (23; kindly provided by Jeff Green, NIH) were grown in DMEM high glucose medium (11995, Invitrogen), supplemented with 10% (v/v) FBS and penicillin/streptomycin. 4T1 cells (2939, ATCC) were maintained in RPMI 1640, 10% FBS, 10 mmol/L HEPES, 100 mmol/L sodium pyruvate and 0.25% glucose. Phoenix Ecotropic packaging cell line (3444, ATCC) and Lenti-X293T packaging cells (632180, Clontech) were maintained in DMEM supplemented with 100 mmol/L sodium pyruvate, 200 mmol/L L-glutamine and non-essential amino acids. Cell lines were authenticated by short tandem repeat (STR), single-nucleotide polymorphism (SNP), and fingerprint analyses and passaged for less than 6 months.

The "Light II" NIH/3T3 cell line stably transfected with a Gli-responsive firefly luciferase reporter and Renilla-luciferase expression vector (CRL-2795, ATCC) was grown in DMEM supplemented with 10% FCS containing 0.1 mg/mL Zeocin, and 0.4 mg/mL Geneticin.

Cell viability assay (MTS assay) was carried out using the CellTiter 96 AQ_{ueous} Cell Proliferation Assay (G5421, Promega) according to the manufacturers recommendation.

Flow cytometry

Tumors were processed into single cell suspensions before staining and fluorescence-activated cell sorting (FACS). Before staining, samples were blocked and then stained with a R-Phycoerythrin (R-PE)–Conjugated Rat anti-Mouse CD24 monoclonal antibody (553262, BD Pharmingen) or the PE Rat IgG2b negative control (122-116-072 Jackson ImmunoResearch) for 30 minutes on ice. Samples were sorted on the FACS Vantage SETM Cell Sorter (with FACSDiVa Option; BD Biosciences) running BD FACSDiVa software version 5.0.3 (BD Biosciences).

Quantitative real-time PCR

cDNA was synthesized using an avian myeloblastosis virus (AMV) reverse transcriptase system (A3500 Promega) as per protocol. Quantitative real-time PCRs (qRT-PCR) were carried out using the Roche Universal Probe Library System on a Roche LightCycler480, 384 well platform, with primers as follows: SHH forward CAA ATT ACA ACC CCG ACA TC, SHH reverse GCA TTT AAC TTG TCT TTG CAC CT, Ptch1 forward GGC CTG GCA GAG GAC TTA C, Ptch1 reverse GGA AGC ACC TTT TGA GTG GA, Ptch2 forward GTC CAC CTA GTG CTC CCA AC, Ptch2 reverse CTC AGC TCC TGA GCC ACA TT, Gli1 forward GGA CCC ACT CCA ATG AGA AG, Gli1 reverse CAT GCA CTG TCT TCA CGT GTT, Hhip forward GTG TTC GGA GAT CGC AAT G, Hhip reverse TTT TCT TGC CAT TGC TTG GT, PECAM1 forward AGC CAG TAG CAT CAT GGT CA, PECAM1 reverse AGC AGG ACA GGT CCA ACA AC, β-actin forward GGA TGC AGA AGG AGA TTA CTG C, β-actin reverse CCA CCG ATC CAC ACA GAG TA.

Further primer details are shown in Supplementary Table S2. The programs used are shown in Supplementary Table S3. Data were analyzed using the comparative C_T method ($\Delta\Delta C_T$).

Expression constructs

The full-length *SHH* cDNA (2,716 bp) was subcloned from pRK5-SHH (24) into pMSCV-puro retroviral expression vector (634401, Clontech). The pLV4301G-enhanced luciferase third generation lentiviral construct was used for *in vivo* imaging and expresses green fluorescent protein (GFP) and luciferase was used for *in vivo* imaging (25). To generate pLV4301G viral stocks, 293T lentiviral packaging cells were transfected as described for the retrovirus production below. 4T1 and M6 cells were infected with the construct and sorted for GFP before expanding for subsequent experiments. For retrovirus production, phoenix-eco cells (26) were seeded at 1.8×10^6 cells/well in 60-mm dishes and transfected with 2 μg of plasmid (SHH or vector alone) and 1 μg of pCL-Eco (12371, Addgene) using Effectene transfection reagent (301425, Qiagen) as directed. Media was changed 24 hours after transfection and a further 24 hours were allowed for virus production. Forty-eight hours posttransfection diluted viral supernatant (1:10 in M6 media containing 8 μg/mL polybrene) was used to infect M6 pLV4301G sorted cells seeded at 0.8×10^5 cells/well in 6-well plates. Transduced cells were selected with 5 μg/mL of puromycin 48 hours after infection. Selection pressure was maintained throughout subsequent passages.

Neutralizing antibody

Hybridomas for hedgehog (clone 5E1) or control antigalactosidase (clone 40-1a) IgG1 monoclonal antibodies were obtained from the Developmental Studies Hybridoma Bank (UIOWA, developed under the auspices of the NICHD and maintained by The University of Iowa). Ultrapure antibodies (0.23EU endotoxin/mg of protein) were generated and purified by the Recombinant Products Facility at the University of New South Wales. Mice were treated twice a week by intraperitoneal (i.p.) injection with either 0.5 mg 5E1 or IgG1 control antibody.

Statistical analyses

Statistical evaluation was carried out using Statview 5.0 Software (Abacus Systems). A value of $P < 0.05$ was accepted as statistically significant. Baseline characteristics of the cohort were defined using simple frequency distributions. Cutoffs for expression of the biological markers examined were determined using an optimal cut-point technique (27).

Multivariate Cox proportional hazards analyses used "backwards" modeling to generate models predictive of outcome. Spearman–Rank correlation was used to explore

Downloaded from cancerres.aacrjournals.org on September 19, 2011
Copyright © 2011 American Association for Cancer Research

DOI:10.1158/0008-5472.CAN-10-3738

the relationship between 2 continuous variables in the human Hh protein expression studies. Simple unpaired *t* tests were used to compare 2 groups in the mouse studies.

Results

Hh ligand is a marker of poor prognosis in invasive ductal carcinoma

We examined our cohort of 292 patients with invasive ductal carcinoma of the breast using rigorously validated antibodies to Hh ligand, Ptch, and Gli1. Examples of the expression of Hh ligand and Gli1 are shown in Figure 1A. Cytoplasmic expression of Hh ligand could be assessed in 279 patients and was present in virtually all cases (275 of 279, 98%) in both the epithelium and the stroma (279 of 279, 100%). However, only 34% (96 of 279) of cases showed high intensity Hh staining in carcinoma cells (Fig. 1A). Kaplan–Meier survival analysis showed that those patients had a poorer outcome in terms of breast cancer metastasis ($P = 0.0004$, HR 1.95, 95% CI 1.2–3.1) and breast cancer–specific death ($P = 0.002$, HR 2.3, 95% CI 1.3–4.0, Fig. 1B). High Hh ligand expression was also associated with grade 3, larger (>20 mm), and more proliferative (high Ki67) tumors, PR negative status (all $P < 0.05$, Table 1), and was strongly correlated with the basal-like subtype of breast cancer ($P = 0.001$). There was no association with any other subtypes. High Hh ligand expression was not independently prognostic in multivariate analysis. There was a strong association between Hh ligand expression and proliferative cell-cycle proteins such as cyclin A (Spearman–Rank correlation Rho = 0.344, $P < 0.0001$), cyclin B1 (Rho = 0.354, $P < 0.0001$) as well as cyclin E1 (Rho = 0.405, $P < 0.0001$). There was no significant association of stromal Hh expression with survival.

Ptch1 was assessable in 197 cases and showed epithelial cytoplasmic expression in 93% of cases (184/197) and stromal cytoplasmic expression in 89%. Univariate analysis for breast cancer–specific death showed no prognostic significance for cytoplasmic epithelial Ptch1 expression ($P = 0.8$) and only a borderline association for stromal Ptch1 ($P = 0.05$).

Both nuclear and cytoplasmic Gli1 were assessed in the cohort but only cytoplasmic Gli1 showed any association with survival. High cytoplasmic stromal Gli1 expression (example shown in Fig. 1A) was determined by optimal cut-point determination as more than 20% of stromal cells expressing Gli1. These Gli1 positive stromal cells had the appearance of fibroblasts based on morphological assessment by a specialist pathologist. There were 83 (31%) stromal Gli1 positive cases, which were associated with breast cancer–specific death ($P = 0.004$, HR 2.4, 95% CI 1.3–4.1) on univariate analysis (Fig. 1B). There was no prognostic significance to nuclear Gli1 expression in either the stroma ($P = 0.8$) or the epithelium ($P = 0.4$) by Kaplan–Meier survival analysis.

In view of the known paracrine mechanism of Hh pathway signaling in development in many organs and in a number of malignancies, we developed a "paracrine" signature defined as cases with both high Hh expression in the epithelium (Hh intensity score 3) and high Gli1 in the stroma (>20% of stromal cells expressing Gli1). This "paracrine" signature identified 16% of cases (44/282) and was independently prognostic in multivariate analysis for overall survival (HR1.7, $P = 0.04$, 95% 1.0–2.8; Table 2; Fig. 1B) and approached significance for breast cancer–specific death ($P = 0.09$) in the resolved model.

Aberrant expression of Hh ligand is an early event in mammary carcinogenesis

In view of our findings of the prognostic significance of Hh ligand expression in invasive ductal carcinoma, we were interested to identify at what stage of breast cancer development Hh ligand expression was first upregulated. We examined expression of Hh ligand using immunohistochemistry in 2 cohorts of preinvasive and malignant breast lesions; a test cohort and a validation cohort both comprising a histological progression series of increasing architectural atypia and malignancy including *in situ* and invasive ductal carcinoma.

We observed a striking, progressive increase in the expression of epithelial Hh ligand in hyperplasia, atypia, and *in situ* malignancy (DCIS) in both the test and validation cohorts (Fig. 1C and D). This was seen in the earliest lesions in the progression series, with greater expression of Hh ligand in histologically normal ducts adjacent to invasive carcinoma compared with normal ducts from reduction mammoplasty patients in the test cohort ($P < 0.05$), with further significant increases in ductal hyperplasia and then DCIS.

There were also incremental increases in Hh ligand expression from low- to intermediate- to high-grade DCIS in the validation cohort. In the test cohort, there was no significant change in the expression of Hh between grade 3 DCIS and invasive carcinoma.

In view of our findings in human tissue, we explored similarities with a mouse model of basal-like mammary carcinoma, in which we could study functional effects of Hh pathway manipulation. We selected the C3(1)/Tag model as it has a well-defined premalignant sequence and gives rise to basal-like tumors (28). In keeping with our human data, we found that lesions of the C3 (1)/Tag model also showed increased expression of Hh ligand in early proliferative lesions (hyperplasia) such that Hh ligand is significantly higher in proliferative and malignant lesions than normal mammary ductal epithelium (Supplementary Fig. S4), supporting the use of this model in subsequent studies of Hh function in mammary carcinoma.

Functional effects of Hh overexpression

In view of our data in human breast cancer showing that high level Hh ligand expression is a marker of poor prognosis, we investigated underlying mechanisms that might contribute to this finding. We elected to use the M6 cell line derived from the C3 (1)/Tag model as a particularly suitable model for *in vivo* and *in vitro* studies. We first determined the effects of Hh overexpression in a transplant model in which M6 cells stably expressing Hh ligand (M6-HH), or controls, were transplanted into the fat pad of immunodeficient $Rag^{-/-}$ mice. M6 cells stably expressing Hh formed significantly larger tumors with a 4-fold increase in mean tumor volume ($P = 0.0006$) and a 3-fold increase in weight compared with controls at endpoint ($P = 0.005$, Fig. 2A). This was confirmed by live imaging studies

Downloaded from cancerres.aacrjournals.org on September 19, 2011
Copyright © 2011 American Association for Cancer Research

DOI:10.1158/0008-5472.CAN-10-3738

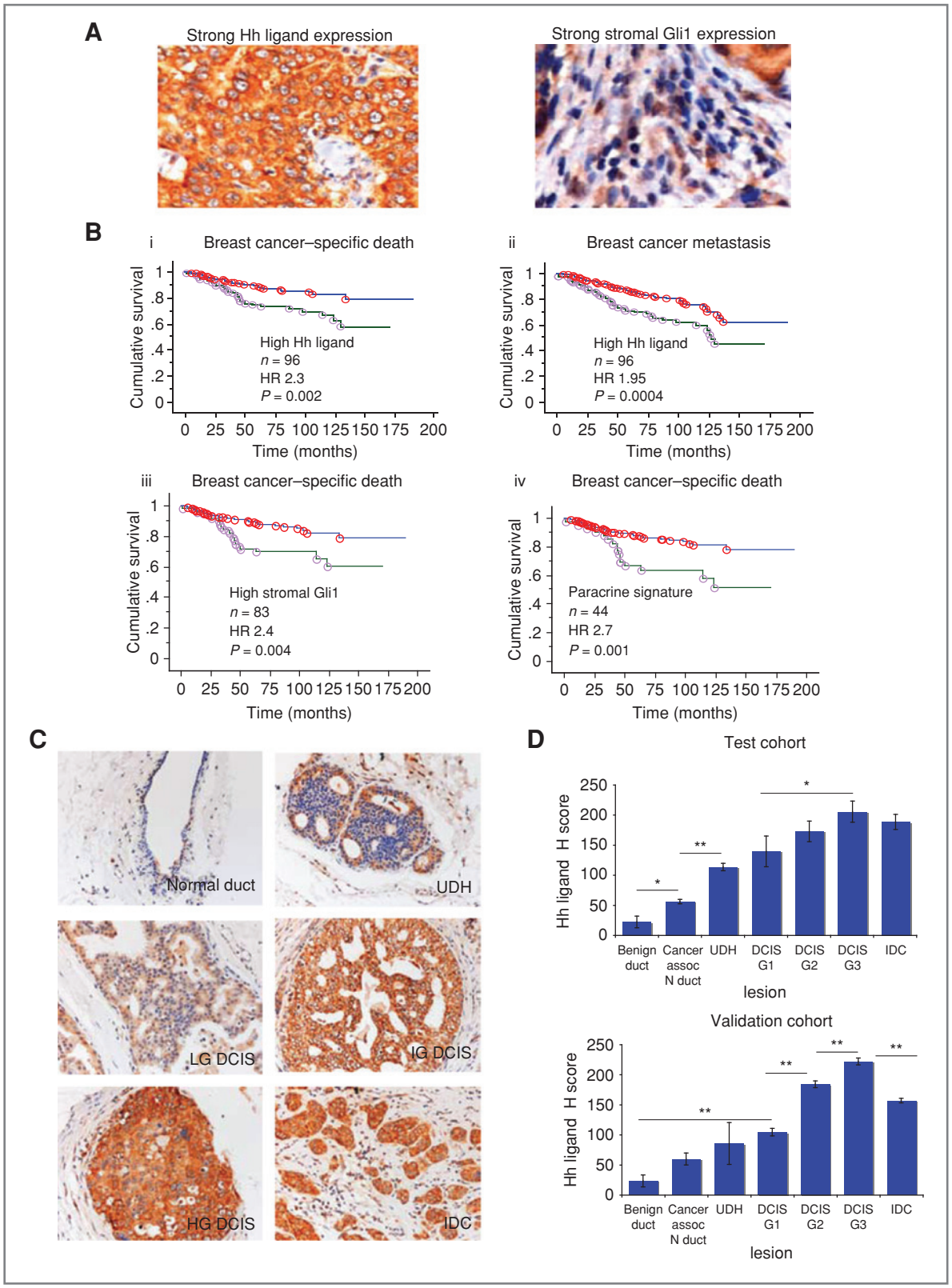

Figure 1. High Hh ligand is associated with a poor prognosis in invasive ductal carcinoma and is an early event in breast cancer progression. A, high Hh ligand expression (400×) and high stromal Gli1 expression (1,000×). B, Kaplan–Meier curves for (i) breast cancer recurrence and (ii) breast cancer–specific death for high Hh, (iii) breast cancer–specific death for high stromal Gli1, and (iv) breast cancer–specific death for the "paracrine" signature. C, increasing intensity of Hh ligand expression in lesions with greater cytological and architectural atypia (all images 200×). UDH, usual ductal hyperplasia; LG, low grade; IG, intermediate grade; HG, high grade; IDC, invasive ductal carcinoma. D, quantitation of Hh staining intensity in 2 independent cohorts of lesions.

Downloaded from cancerres.aacrjournals.org on September 19, 2011
Copyright © 2011 American Association for Cancer Research

DOI:10.1158/0008-5472.CAN-10-3738

Table 1. Clinicopathologic associations of Hh overexpression

Clinicopathologic parameter	Total $N = 279$	Hh high $N = 96$ (34%) n (%)	Hh low $N = 183$ (66%) n (%)	P^a
Median, y (range): 55 (24–87)				0.03
Age ≥55 y	127	53 (42)	74 (58)	
Age <55 y	152	43 (28)	109 (72)	
Median size, mm (range): 21 (0.9–80)				0.01
Size ≥20 mm	115	50 (43)	65 (57)	
Size <20 mm	164	46 (28)	118 (72)	
Grade				<0.0001
3	126	61 (48)	65 (52)	
1 and 2	153	35 (23)	118 (77)	
Lymph node status				0.01
Positive	121	52 (43)	69 (57)	
Negative	155	44 (28)	111 (72)	
Estrogen receptor				0.07
Positive	187	58 (31)	129 (69)	
Negative	88	38 (43)	50 (57)	
Progesterone receptor				0.03
Positive	158	46 (29)	112 (71)	
Negative	118	50 (42)	68 (58)	
HER2 status				0.99
Positive	51	17 (33)	34 (67)	
Negative	217	75 (35)	142 (65)	
Ki67 > median				0.0001
High	121	58 (47)	63 (53)	
Low	127	31 (24)	96 (75)	

[a] χ^2 analysis P value.

Table 2. Univariate and multivariate analysis of clinicopathologic variables for overall survival

Variable	HR (95% CI)	P
A, Univariate analysis		
Histological grade 3	3.8 (2.1–7.0)	<0.0001
Size > 20 mm	2.4 (1.6–3.7)	<0.0001
Lymph nodes > 0	3.3 (1.9–6.0)	<0.0001
ER positive	0.4 (0.3–0.6)	<0.0001
PR positive	0.3 (0.2–0.6)	<0.0001
HER2 positive	2.3 (1.8–5.8)	<0.0001
Epithelial Hh high	2.3 (1.3–4.0)	0.002
Stromal Gli1 high	2.4 (1.3–4.1)	0.004
Paracrine Hh signature	2.7 (1.5–4.8)	0.001
B, Multivariate analysis, resolved model		
Lymph nodes > 0	2.2 (1.3–3.6)	0.001
PR positive	0.3 (0.2–0.7)	0.0002
HER2 positive	1.9 (1.1–3.2)	0.02
Paracrine Hh signature	1.7 (1.01–2.8)	0.04

using luciferase expression which showed greater signal in the Hh overexpressing tumors compared with controls (Fig. 2B). Ninety days after transplantation, no mice carrying Hh-overexpressing tumors ($N = 8$) survived, compared with 88% survival for mice bearing control tumors ($N = 8$; $P < 0.0004$). There were also significant differences in the local invasion of the 2 groups. Control tumors were adherent to the overlying skin but showed well defined edges. In contrast, the Hh overexpressing tumors were locally very aggressive, invading through the abdominal musculature, and penetrating the peritoneal cavity (Fig. 2C).

Histological analysis showed that 4 of 5 (80%) of Hh overexpressing tumors showed invasion of lymphatic spaces by tumor cells, confirmed by LYVE-1 immunohistochemistry (Fig. 2D), compared with only 1 of 5 in the control group.

We further explored this model to investigate the phenotype of M6-HH and M6-control tumors matched for size before they became large and necrotic. Although there was no difference in the incidence of peritumoral lymphatic invasion (data not shown) when tumors were of an equivalent size, Hh overexpressing tumors were denser and were histologically less well differentiated, with no glandular structures observed

Downloaded from cancerres.aacrjournals.org on September 19, 2011
Copyright © 2011 American Association for Cancer Research

DOI:10.1158/0008-5472.CAN-10-3738

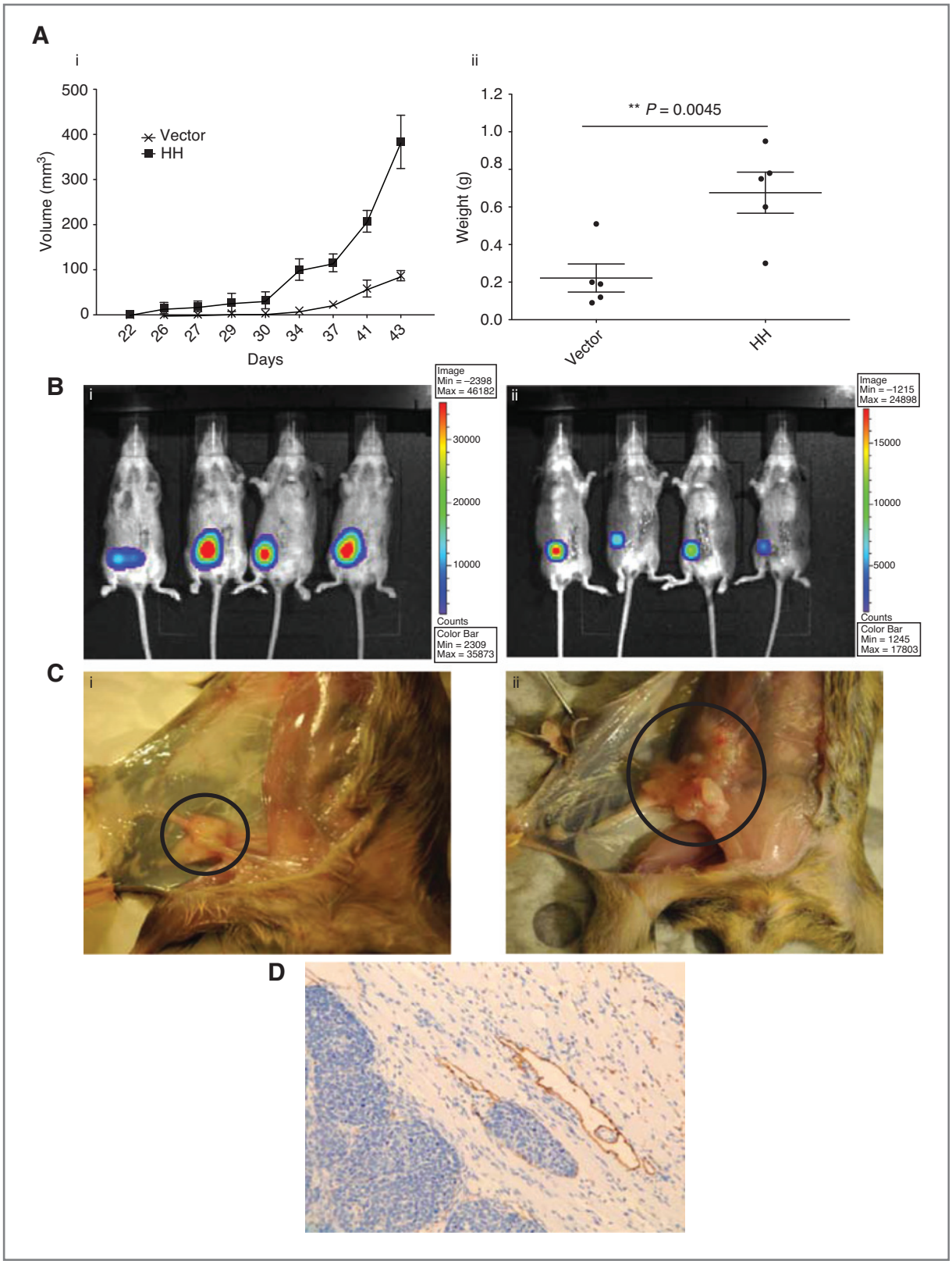

Figure 2. Hh overexpression promotes tumor growth, local aggressiveness, and lymphatic invasion and is associated with poor survival. A, M6-HH allografts show increased tumor volume and a 3-fold increase in tumor weight at endpoint. B, luciferase activity of M6 tumors *in vivo*. M6-HH tumors (left) show larger signals than controls (right). C, control tumors show limited local invasion and are confined to the overlying skin (left, tumor highlighted by black circle), whereas M6-HH tumors (right) show marked local invasion, growing through the abdominal wall and penetrating the peritoneal cavity. D, M6-HH tumors show increased peritumoral lymphatic invasion (LYVE-1 immunohistochemistry, 100×).

Downloaded from cancerres.aacrjournals.org on September 19, 2011
Copyright © 2011 American Association for Cancer Research

DOI:10.1158/0008-5472.CAN-10-3738

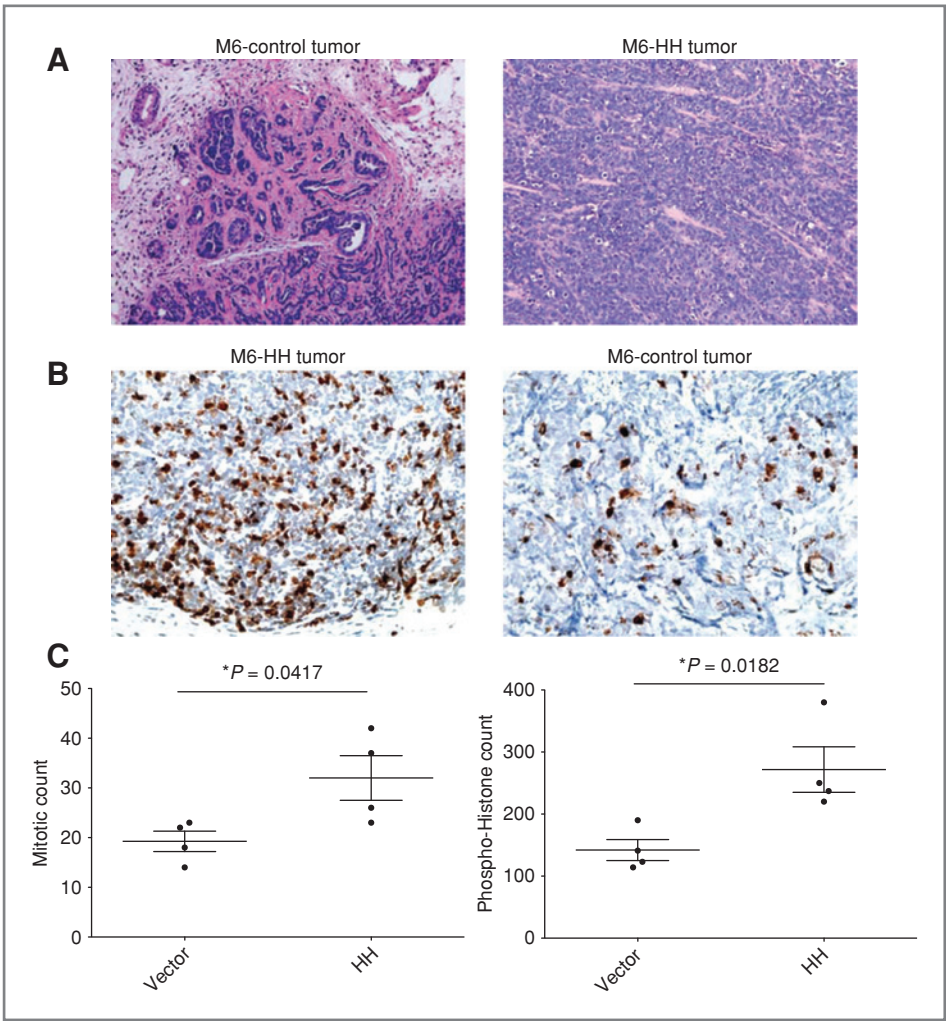

Figure 3. Hh overexpression results in more poorly differentiated and more proliferative tumors. A, control tumors of equivalent volume to M6-HH tumors show better differentiation with well developed glandular structures and more stroma. In contrast M6-HH tumors (right) show no glandular differentiation and very little stroma, consisting of sheets of poorly differentiated malignant cells (H&E 200×). B, phospho-histone H3 immunohistochemistry in M6-HH tumors compared with control tumors (200×). C, M6-HH tumors have higher mitotic counts (left) and phospho-histone H3 counts (right).

in any Hh tumors compared with glandular structure observed in all of vector controls (Fig. 3A). We observed no difference in tumor infiltration by inflammatory cells (data not shown, assessed by IF for CD45 and F4/80), microvessel density (data not shown, assessed by CD31 IF) or in apoptosis (assessed by caspase-3 IF, data not shown). However, there was a significant increase in tumor cell proliferative fraction with a 2-fold higher proportion of phospho-histone H3-positive cells per hpf in the Hh expressing tumors compared with vector controls of the same size (Fig. 3B and C). Mitotic counts (per 10 hpf) were also 50% higher in the Hh-positive tumors compared with vector controls of the same size (Fig. 3C).

A stromal requirement for Hh-mediated tumor growth

We confirmed M6 cells with Hh produced functional ligand using a Gli1 luciferase reporter, the "light II assay." This activity could be blocked by 5E1 an anti-Hh blocking antibody that inhibits binding of all 3 ligands to the Ptch receptor, but not by control antibody (Fig. 4A). Using these cells, we then conducted detailed *in vitro* studies to investigate possible mechanisms for the differences in tumor growth observed in the *in vivo* studies. Based on our observation of increased proliferation in M6-HH tumors, we hypothesized that M6-HH would proliferate faster than control cells. However, *in vitro* MTS assays showed no difference in the growth curves (Fig. 4B). We also speculated that in view of its known role in stem cell regulation (5), Hh might promote increased self-renewal capacity. However, modified "mammosphere" assays showed no difference in sphere forming capacity between control or M6-HH cells in primary, secondary, or tertiary cultures (data not shown). Furthermore, inhibition of Hh signaling with 5E1 antibody also had no effect on the development of primary or secondary mammospheres between the 2 groups (data not shown). Finally, we found no difference in migration of M6-HH cells *in vitro* compared with vector control M6 cells (data not shown).

These findings suggest that there may be a critical stromal interaction to account for the dramatic difference in tumor growth seen with Hh overexpression. We further explored this by carrying out quantitative PCR (qPCR) for key Hh pathway components, including readouts of canonical signaling; *Hhip*, *Ptch1*, *Ptch2*, and *Gli1*. There was no change in the expression

Downloaded from cancerres.aacrjournals.org on September 19, 2011
Copyright © 2011 American Association for Cancer Research

DOI:10.1158/0008-5472.CAN-10-3738

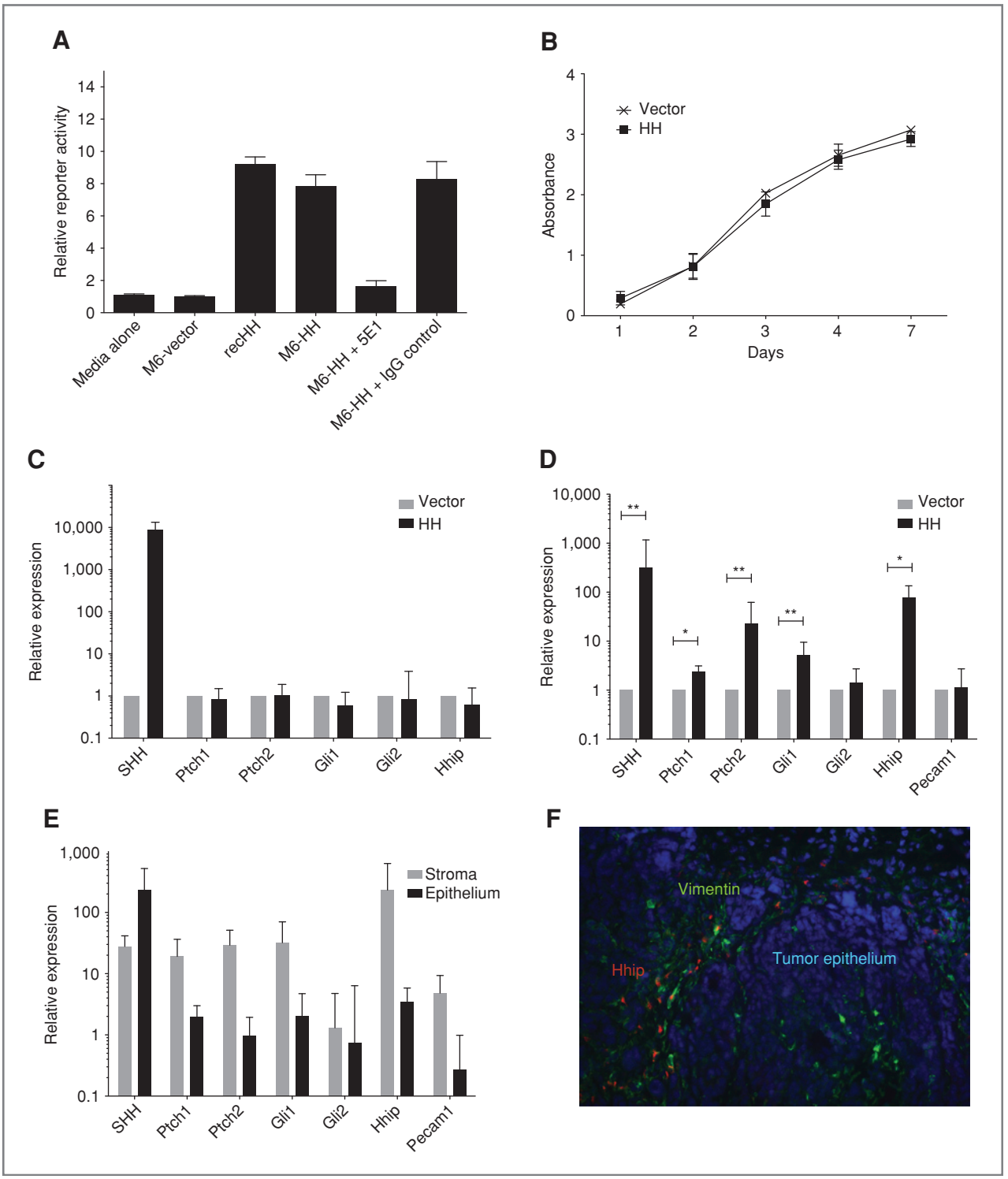

Figure 4. Hh-mediated growth requires stromal interaction. A, light II luciferase assay showing M6-HH cells produce functional Hh ligand which can be blocked by 5E1, but not by the control antibody. Recombinant Hh ligand is used as a positive control. B, M6 cells show no differences in growth measured by MTS assay with and without HH overexpression. C, qPCR for *HH* genes showing no change in pathway genes compared with vector controls except for SHH in the HH cells in culture. D, qPCR for *HH* genes in whole tumors showing increased *HH* responsive genes. E, qPCR for *HH* genes in separated epithelium and stroma in M6-HH tumors. SHH as expected is seen at highest levels in the epithelium, whereas *HH* responsive genes induced by HH overexpression are observed at highest levels in the stroma. F, dual immunofluorescence for vimentin (green) and Hhip (red). Nuclei are shown in blue (DAPI) with densely packed nuclei within the epithelial compartment. Hhip expression is not seen in the tumor epithelium but only in the peritumoral fibroblasts highlighted by vimentin expression (200×). *, $P < 0.05$; **, $P < 0.01$.

Downloaded from cancerres.aacrjournals.org on September 19, 2011
Copyright © 2011 American Association for Cancer Research

DOI:10.1158/0008-5472.CAN-10-3738

of any hedgehog pathway genes in the M6-HH cells in culture compared with controls except for SHH as expected (Fig. 4C). However, there was a significant increase in *Hhip* ($P = 0.014$), *Ptch1* ($P = 0.023$), *Ptch2* ($P = 0.009$), and *Gli1* ($P = 0.009$) mRNA in Hh overexpressing tumors compared with control (Fig. 4D). To identify in which compartment these changes occurred we separated the stroma and epithelium of the M6-HH tumor using FACS sorting for CD24 (a marker of epithelium; ref. 29). These studies revealed upregulation of *Ptch1*, *Ptch2*, *Gli1*, and *Hhip* expression exclusively in the stromal compartment compared with the epithelium (Fig. 4E). The epithelial compartment showed only upregulation of Shh as expected. These findings were further validated using indirect double immunofluorescence on the tumor samples. Hhip expression was confined to peritumoral stromal fibroblasts (confirmed by vimentin expression, Fig. 4F) with no expression in the epithelial cells (data not shown, keratin immunostaining) or inflammatory cells (data not shown, CD45 immunostaining) and was not seen in the control tumors (data not shown). These data confirm that there is upregulation of downstream Hh pathway components predominantly in the stroma in response to Hh produced by the epithelium, supporting a paracrine signaling mechanism in our model of mammary carcinoma.

Hh blockade inhibits tumor growth and metastasis

In view of our data showing that Hh overexpressing tumors were associated with larger, more poorly differentiated tumors with an increased rate of lymphatic invasion, we investigated the functional requirements for Hh ligand in the development of tumor growth and metastatic dissemination. Using the M6-HH allograft model, we treated mice with twice weekly intraperitoneal injections of either 5E1 or a control antibody. The ability of 5E1 to inhibit Hh signaling was confirmed by qPCR in tumor samples showing marked inhibition of *Hhip* expression in the treatment group (Fig. 5A). The 5E1 treated mice ($N = 10$) showed a markedly slower rate of tumor growth (Fig. 5B) and also had statistically significant longer median survival times (>110 days compared with 78 days, $P = 0.0002$) than the control antibody treated group ($N = 5$; Fig. 5C). In addition, *ex vivo* imaging and histological analysis of harvested organs showed a difference in the pattern of metastatic disease between control and treated groups. Although all mice in both groups developed lung metastases equivalently, 100% of control mice developed metastases to the liver and pancreas (Fig. 5D), but only 25% of 5E1 treated mice developed liver metastases, and none developed pancreatic metastases. These data suggested that Hh played a role in the development of metastatic disease.

We next sought to independently validate these findings in the well-characterized 4T1 allograft model (25), which rapidly develops spontaneous metastases. qPCR showed that *HH* pathway genes, including all 3 Hh ligands were expressed in untreated 4T1 cells (data not shown), confirming it is a good model in which to investigate the effects of HH inhibition. We transplanted the same number of 4T1 cells into the fat pads of immunocompetent BALB/c mice followed by twice weekly treatment with intraperitoneal 5E1 or control antibody. There was no apparent growth or histological differences in the primary tumors (data not shown). However, the size of metastatic deposits was smaller in the 5E1 treatment group ($P = 0.02$, Fig. 5E), suggesting that Hh controls the proliferation of primary and metastatic tumors.

Discussion

The importance of Hh signaling in a subset of common human cancers is thought to rest on its ability to recreate developmental epithelial–mesenchymal paracrine signaling (30) where the signal from Hh ligand expressed by tumor cells is received by the receptor Ptch in the adjacent stroma (8–10, 31, 32). Our study represents the first detailed description of the localization of key Hh pathway components in a large, well-characterized breast cancer cohort using rigorously validated antibodies. For the first time, we also report that the expression of Hh ligand in the epithelial cells of breast cancer is associated with increased risk of metastasis, breast cancer–specific death, and a more proliferative, aggressive, basal-like phenotype and that Hh ligand expression increases during progression of premalignant breast epithelial lesions. Taken together, these data strongly suggest the Hh ligands play a role in the progression and invasiveness of a subset of breast cancers.

Our data support a paracrine mode of canonical Hh signaling in breast cancer, although we cannot exclude a cell-autonomous role for Hh signaling in a small subset of tumors, or within a small population of tumor cells within a given tumor. In keeping with previously reported smaller studies (4, 13, 16), we found expression of Ptch and Gli1 in breast cancer specimens. Our data show that a combination of high Hh ligand in the epithelium and Gli1 in the stroma, a "paracrine" pattern, is independently prognostic for overall survival and approaches significance for breast cancer–specific death. The importance of this "paracrine" Hh signature is supported by evidence that Hh target gene expression is limited to the stromal compartment in mouse models, and that Hh ligand expression produces no detectable cell-autonomous effect in mammary carcinoma cells *in vitro*. Recent studies show that Hh signaling may be important in cellular responses in endothelial and mesenchymal cells (33, 34), adding weight to the idea that Hh ligand can drive the formation of an optimal stromal environment in some solid tumors. Our data also show that inhibition of the stromal Hh response, rather than direct targeting of neoplastic cells, is a new potential therapeutic approach.

By manipulating the expression and/or activity of Hh ligand in breast cancer cells *in vivo*, we have also shown the functional significance of this pathway in a model that closely resembles basal-like breast cancer. The marked effect of Hh expression on tumor growth, grade, histology, and metastatic potential in these models are remarkably consistent with our data in human breast cancer. Interestingly, blockade of Hh signaling *in vivo* altered not only the size of metastases but also their tissue profile, suggesting that Hh signaling may also act to promote organ-specific growth based on selection for more favorable microenvironments.

Downloaded from cancerres.aacrjournals.org on September 19, 2011
Copyright © 2011 American Association for Cancer Research

DOI:10.1158/0008-5472.CAN-10-3738

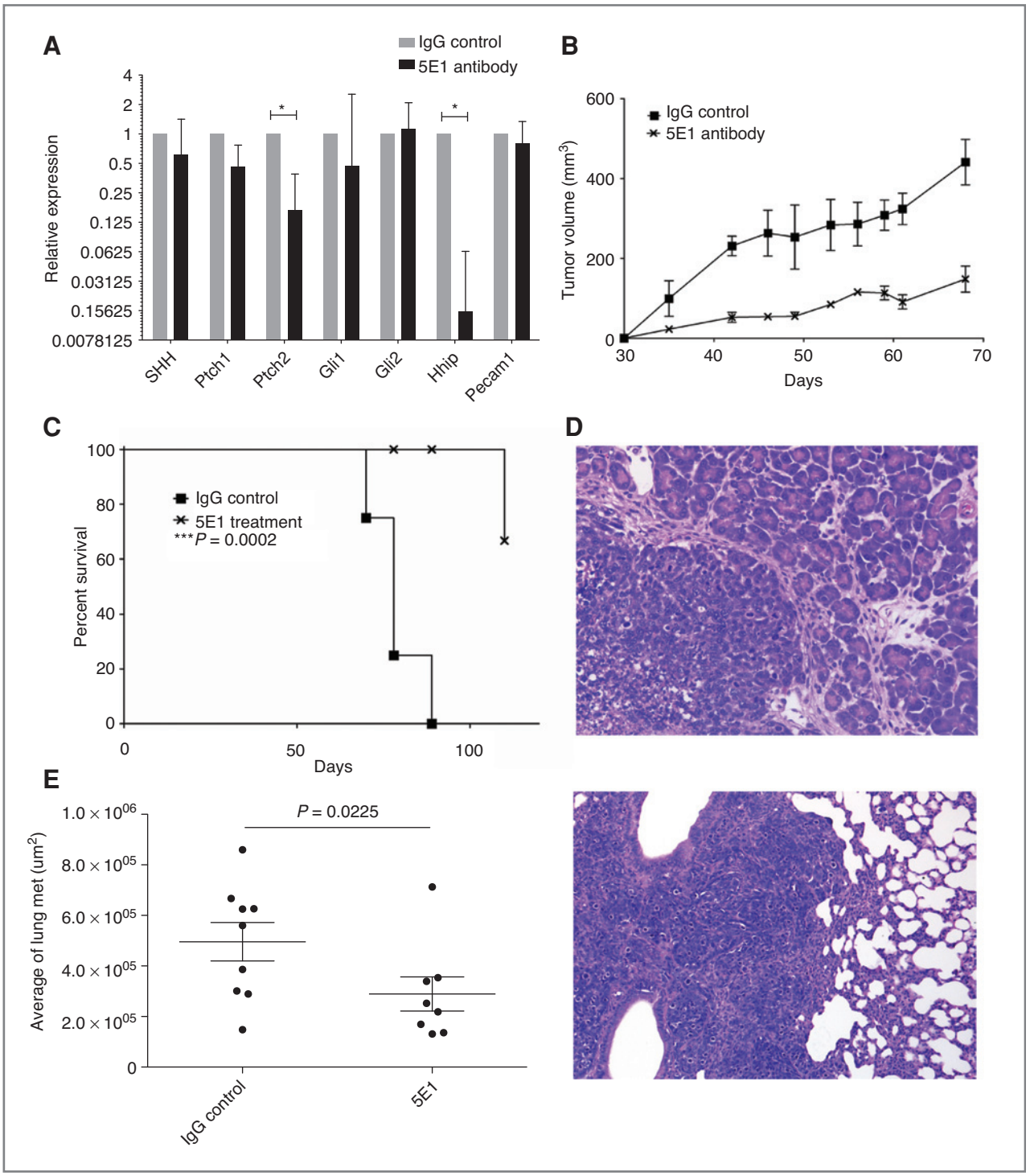

Figure 5. Hh inhibition decreases tumor growth and reduces the size of lung metastases. A, qPCR for *HH* genes showing inhibition of key readouts of Hh pathway activity with 5E1 treatment. B, M6-HH tumors show reduced growth rates *in vivo* with 5E1 treatment in comparison to the control antibody. C, M6-HH tumors treated with 5E1 show significantly longer survival compared with those treated with control antibody. D, representative pancreatic metastasis in M6-HH mouse (H&E, 200×). E, Hh inhibition with 5E1 decreases the size of lung metastatic deposits in 4T1 allografts compared with control antibody treated shown graphically (left; *, $P < 0.05$) with an example of a lung metastasis in this model shown at right.

The clinical implications of these findings for breast cancer include (i) a biological and functional connection between Hh ligand expression and basal-like breast cancer, (ii) a potential treatment for basal-like breast cancer for which there is no effective targeted therapy, and (iii) the importance of epithelial interactions as potential therapeutic targets. The development

Downloaded from cancerres.aacrjournals.org on September 19, 2011
Copyright © 2011 American Association for Cancer Research

DOI:10.1158/0008-5472.CAN-10-3738

of therapeutics directed at stromal Hh signaling may represent a novel approach to the treatment of locally advanced or metastatic breast cancer.

Disclosure of Potential Conflicts of Interest

No potential conflicts of interest were disclosed.

Acknowledgments

5E1 hybridomas were obtained from the University of Iowa Hybridoma Bank. Some tissues were also received from the Australia Breast Cancer Tissue Bank. The authors thank the assistance of Ms. Alice Boulghourjian and Ms. Sarah Eggleton with immunohistochemistry, Ms. Anne Holliday for data management, Dr. Samantha Oakes for providing mouse tissue, and Mrs. Gillian Lehrbach with cell culture. The authors also thank Prof. Roger Daly and Dr. Elizabeth Caldon for their advice on the manuscript.

Grant Support

Australia Breast Cancer Tissue Bank is generously supported by the National Health and Medical Research Council of Australia, The Cancer Institute NSW, and the National Breast Cancer Foundation. This work was supported by the following grants: the National Health and Medical Research Council (grant nos. 481378 (S.A. O'Toole), 427601 (R.L. Sutherland) and 535947 (S.A. O'Toole, A. Swarbrick, D.N. Watkins), the Cancer Institute NSW [grant nos. 08/ECF/1–12 (A. Swarbrick), 07/CRF/1–06 (S.A. O'Toole), and 07-CDF-1/28 (E.A. Musgrove)], the St Vincent's Clinic Foundation, the National Breast Cancer Foundation, the Australian Cancer Research Foundation, the RT Hall Trust, and the Petre Foundation.

The costs of publication of this article were defrayed in part by the payment of page charges. This article must therefore be hereby marked *advertisement* in accordance with 18 U.S.C. Section 1734 solely to indicate this fact.

Received October 14, 2010; revised February 4, 2011; accepted March 8, 2011; published online June 1, 2011.

References

1. Peto R, Boreham J, Clarke M, Davies C, Beral V. UK and USA breast cancer deaths down 25% in year 2000 at ages 20–69 years. Lancet 2000;355:1822.
2. Viani GA, Afonso SL, Stefano EJ, De Fendi LI, Soares FV. Adjuvant trastuzumab in the treatment of her-2-positive early breast cancer: a meta-analysis of published randomized trials. BMC Cancer 2007;7:153.
3. Rakha EA, Reis-Filho JS, Ellis IO. Basal-like breast cancer: a critical review. J Clin Oncol 2008;26:2568–81.
4. Kubo M, Nakamura M, Tasaki A, Yamanaka N, Nakashima H, Nomura M, et al. Hedgehog signaling pathway is a new therapeutic target for patients with breast cancer. Cancer Res 2004;64:6071–4.
5. Liu S, Dontu G, Mantle ID, Patel S, Ahn NS, Jackson KW, et al. Hedgehog signaling and Bmi-1 regulate self-renewal of normal and malignant human mammary stem cells. Cancer Res 2006;66:6063–71.
6. Fiaschi M, Rozell B, Bergstrom A, Toftgard R. Development of mammary tumors by conditional expression of GLI1. Cancer Res 2009;69:4810–7.
7. Ingham PW, McMahon AP. Hedgehog signaling in animal development: paradigms and principles. Genes Dev 2001;15:3059–87.
8. Shaw A, Gipp J, Bushman W. The Sonic Hedgehog pathway stimulates prostate tumor growth by paracrine signaling and recapitulates embryonic gene expression in tumor myofibroblasts. Oncogene 2009;28:4480–90.
9. Tian H, Callahan CA, DuPree KJ, Darbonne WC, Ahn CP, Scales SJ, et al. Hedgehog signaling is restricted to the stromal compartment during pancreatic carcinogenesis. Proc Natl Acad Sci U S A 2009;106:4254–9.
10. Yauch RL, Gould SE, Scales SJ, Tang T, Tian H, Ahn CP, et al. A paracrine requirement for hedgehog signalling in cancer. Nature 2008;455:406–10.
11. Lauth M, Toftgard R. Non-canonical activation of GLI transcription factors: implications for targeted anti-cancer therapy. Cell Cycle 2007;6:2458–63.
12. Lewis MT, Ross S, Strickland P, Sugnet CW, Jimenez E, Scott MP, et al. Defects in mouse mammary gland development caused by conditional haploinsufficiency of Patched-1. Development 1999;126:5181–93.
13. Moraes RC, Zhang X, Harrington N, Fung JY, Wu MF, Hilsenbeck SG, et al. Constitutive activation of smoothened (SMO) in mammary glands of transgenic mice leads to increased proliferation, altered differentiation and ductal dysplasia. Development 2007;134:1231–42.
14. Lewis MT, Ross S, Strickland PA, Sugnet CW, Jimenez E, Hui C, et al. The Gli2 transcription factor is required for normal mouse mammary gland development. Dev Biol 2001;238:133–44.
15. Mukherjee S, Frolova N, Sadlonova A, Novak Z, Steg A, Page GP, et al. Hedgehog signaling and response to cyclopamine differ in epithelial and stromal cells in benign breast and breast cancer. Cancer Biol Ther 2006;5:674–83.
16. Wolf I, Bose S, Desmond JC, Lin BT, Williamson EA, Karlan BY, et al. Unmasking of epigenetically silenced genes reveals DNA promoter methylation and reduced expression of PTCH in breast cancer. Breast Cancer Res Treat 2007;105:139–55.
17. Lopez-Knowles E, O'Toole SA, McNeil CM, Millar EK, Qiu MR, Crea P, et al. PI3K pathway activation in breast cancer is associated with the basal-like phenotype and cancer-specific mortality. Int J Cancer; 126:1121–31.
18. Lopez-Knowles E, Zardawi SJ, McNeil CM, Millar EK, Crea P, Musgrove EA, et al. Cytoplasmic localization of beta-catenin is a marker of poor outcome in breast cancer patients. Cancer Epidemiol Biomarkers Prev; 19:301–9.
19. Millar EK, Anderson LR, McNeil CM, O'Toole SA, Pinese M, Crea P, et al. BAG-1 predicts patient outcome and tamoxifen responsiveness in ER-positive invasive ductal carcinoma of the breast. Br J Cancer 2009;100:123–33.
20. Alle KM, Henshall SM, Field AS, Sutherland RL. Cyclin D1 protein is overexpressed in hyperplasia and intraductal carcinoma of the breast. Clin Cancer Res 1998;4:847–54.
21. Zardawi SJ, Zardawi I, McNeil C, Millar EK, McLeod D, Morey AL, et al. High Notch1 protein expression is an early event in breast cancer development and is associated with the HER-2 molecular subtype. Histopathology 2010;56:286–96.
22. Cheang MC, Voduc D, Bajdik C, Leung S, McKinney S, Chia SK, et al. Basal-like breast cancer defined by five biomarkers has superior prognostic value than triple-negative phenotype. Clin Cancer Res 2008;14:1368–76.
23. Holzer RG, MacDougall C, Cortright G, Atwood K, Green JE, Jorcyk CL. Development and characterization of a progressive series of mammary adenocarcinoma cell lines derived from the C3(1)/SV40 Large T-antigen transgenic mouse model. Breast Cancer Res Treat 2003;77:65–76.
24. Maity T, Fuse N, Beachy PA. Molecular mechanisms of Sonic hedgehog mutant effects in holoprosencephaly. Proc Natl Acad Sci U S A 2005;102:17026–31.
25. Tao K, Fang M, Alroy J, Sahagian GG. Imagable 4T1 model for the study of late stage breast cancer. BMC Cancer 2008;8:228.
26. Pear WS, Nolan GP, Scott ML, Baltimore D. Production of high-titer helper-free retroviruses by transient transfection. Proc Natl Acad Sci U S A 1993;90:8392–6.
27. Harvey JM, Clark GM, Osborne CK, Allred DC. Estrogen receptor status by immunohistochemistry is superior to the ligand-binding assay for predicting response to adjuvant endocrine therapy in breast cancer. J Clin Oncol 1999;17:1474–81.
28. Herschkowitz JI, Simin K, Weigman VJ, Mikaelian I, Usary J, Hu Z, et al. Identification of conserved gene expression features between murine mammary carcinoma models and human breast tumors. Genome Biol 2007;8:R76.
29. Sleeman KE, Kendrick H, Ashworth A, Isacke CM, Smalley MJ. CD24 staining of mouse mammary gland cells defines luminal epithelial, myoepithelial/basal and non-epithelial cells. Breast Cancer Res 2006;8:R7.

Downloaded from cancerres.aacrjournals.org on September 19, 2011
Copyright © 2011 American Association for Cancer Research

DOI:10.1158/0008-5472.CAN-10-3738

30. Litingtung Y, Lei L, Westphal H, Chiang C. Sonic hedgehog is essential to foregut development. Nat Genet 1998;20:58–61.
31. Fan L, Pepicelli CV, Dibble CC, Catbagan W, Zarycki JL, Laciak R, et al. Hedgehog signaling promotes prostate xenograft tumor growth. Endocrinology 2004;145:3961–70.
32. Zhang J, Lipinski RJ, Gipp JJ, Shaw AK, Bushman W. Hedgehog pathway responsiveness correlates with the presence of primary cilia on prostate stromal cells. BMC Dev Biol 2009;9:50.
33. Nakamura K, Sasajima J, Mizukami Y, Sugiyama Y, Yamazaki M, Fujii R, et al. Hedgehog promotes neovascularization in pancreatic cancers by regulating Ang-1 and IGF-1 expression in bone-marrow derived pro-angiogenic cells. PLoS One 5:e8824.
34. Yamazaki M, Nakamura K, Mizukami Y, Ii M, Sasajima J, Sugiyama Y, et al. Sonic hedgehog derived from human pancreatic cancer cells augments angiogenic function of endothelial progenitor cells. Cancer Sci 2008;99:1131–8.

Downloaded from cancerres.aacrjournals.org on September 19, 2011
Copyright © 2011 American Association for Cancer Research

DOI:10.1158/0008-5472.CAN-10-3738

Cancer Research

Hedgehog Overexpression Is Associated with Stromal Interactions and Predicts for Poor Outcome in Breast Cancer

Sandra A. O'Toole, Dorothy A. Machalek, Robert F. Shearer, et al.

Cancer Res 2011;71:4002-4014. Published online May 31, 2011.

Updated Version	Access the most recent version of this article at: doi:10.1158/0008-5472.CAN-10-3738
Supplementary Material	Access the most recent supplemental material at: http://cancerres.aacrjournals.org/content/suppl/2011/04/22/0008-5472.CAN-10-3738.DC1.html

Cited Articles	This article cites 31 articles, 14 of which you can access for free at: http://cancerres.aacrjournals.org/content/71/11/4002.full.html#ref-list-1

E-mail alerts	Sign up to receive free email-alerts related to this article or journal.
Reprints and Subscriptions	To order reprints of this article or to subscribe to the journal, contact the AACR Publications Department at pubs@aacr.org.
Permissions	To request permission to re-use all or part of this article, contact the AACR Publications Department at permissions@aacr.org.

Downloaded from cancerres.aacrjournals.org on September 19, 2011
Copyright © 2011 American Association for Cancer Research